Predicting Alzheimer's disease using combined imaging-whole genome SNP data

Dehan Kong*, Ph.D, K. S. Giovanello†,§, Ph.D, Y.L. Wang‖, Ph.D, Weili Lin‡,§, Ph.D, Eunjee Lee ¶, M.S., Yong Fan**, Ph.D P. Murali Doraiswamy††,MD, and Hongtu Zhu*,‡,§,, Ph.D

for the Alzheimer's Disease Neuroimaging Initiative

* Department of Biostatistics, UNC

† Department of Psychology, UNC

‡ Department of Radiology, UNC

§ Biomedical Research Imaging Center, UNC

¶ Department of Statistics, UNC

‖ School of Computing, Informatics, and Decision Systems Engineering, Arizona State University

** Department of Radiology, University of Pennsylvania

†† Departments of Psychiatry and Duke Institute for Brain Sciences, Duke University

Correspondence to: Hongtu Zhu.

Address: 3105-C McGavran-Greenberg Hall,
UNC Gillings School of Global Public Health, 135 Dauer Drive,
Campus Box 7420,
Chapel Hill, 27599-7420,
USA

Fax: 919-966-3804; phone: 919-966-7272

Email: htzhu@email.unc.edu

Author disclosures are listed at the end of the paper.

The first two authors, Drs. Kong and Giovanello contributed equally to this paper. The last two authors, Drs. Doraiswamy and Zhu, are senior authors of this paper.

ABSTRACT

Background: Less is known about whether both whole genome SNP data and whole brain imaging data offer predictive values to identify subjects at risk for progressing to AD.

Methods: In 343 subjects with mild cognitive impairment (MCI) enrolled in the Alzheimer's Disease Neuroimaging Initiative (ADNI-1), we extracted high dimensional MR imaging (volumetric data on 93 brain regions plus a surface fluid registration based hippocampal subregion and surface data), and whole genome data (504,095 SNPs), as well as routine neurocognitive and clinical data at baseline. MCI patients were then followed over 48 months, with 150 participants progressing to AD.

Results: The model combining just routine clinical and cognitive data with a single genotype (ApoE4) had a low predictive value at 48 months (AUC 0.75). In contrast, the model combining full genetic SNP and imaging data (but without any cognitive data) had a much higher predictive value (AUC 0.95).

Conclusions: It is important to consider the joint effects of both imaging and genetics instead of just considering clinical and cognitive data when predicting the MCI to AD progression.

Keywords: Alzheimer, hippocampal surface, mild cognitive impairment, receiver operating characteristic, whole genome.

1. Background

The growing public threat of Alzheimer's disease (AD) has raised the urgency to discover and validate prognostic biomarkers that may identify subjects at greatest risk for future cognitive decline and accelerate the testing of preventive strategies [1][2]. In this regard, studies of combinatorial biomarkers may have greater ability to capture the heterogeneity and multifactorial complexity of AD, than a traditional single biomarker study [3].

Prior studies of subjects at risk for AD have examined the utility of various individual biomarkers, such as cognitive tests, fluid markers, imaging measures and some individual genetic markers (e.g. ApoE4) [1]. In particular, imaging markers such as hippocampal volume and shape, cortical regional volumes and thickness, and PET (amyloid imaging, FDG) abnormalities have all been linked in one or more studies to faster progression in at risk subjects [4-16], but are not yet optimally predictive at an individual level.

More recently, genome-wide association study (GWAS) data has been used to characterize several potential genetic risk factors for AD with several cross-sectional studies also correlating these data with imaging and fluid biomarkers [17]. However, no prior study, to our knowledge, has leveraged both GWAS SNP data, as well as high dimensional whole brain imaging data to examine their combined value in identifying subjects at greatest risk for progressing to AD.

2. Methods

2.1 *Subjects*

2.1.1 Alzheimer's Disease Neuroimaging Initiative. ``Data used in the preparation of this article were obtained from the Alzheimer's Disease Neuroimaging Initiative (ADNI) database (www.loni.usc.edu/ADNI). The ADNI was launched in 2003 by the National Institute on Aging

(NIA), the National Institute of Biomedical Imaging and Bioengineering (NIBIB), the Food and Drug Administration (FDA), private pharmaceutical companies and non-profit organizations, as a $60 million, 5-year public private partnership. The primary goal of ADNI has been to test whether serial magnetic resonance imaging (MRI), positron emission tomography (PET), other biological markers, and clinical and neuropsychological assessment can be combined to measure the progression of mild cognitive impairment (aMCI) and early Alzheimer's disease (AD). Determination of sensitive and specific markers of very early AD progression is intended to aid researchers and clinicians to develop new treatments and monitor their effectiveness, as well as lessen the time and cost of clinical trials. The Principal Investigator of this initiative is Michael W. Weiner, M.D., VA Medical Center and University of California - San Francisco. ADNI is the result of efforts of many co-investigators from a broad range of academic institutions and private corporations, and subjects have been recruited from over 50 sites across the U.S. and Canada. The initial goal of ADNI was to recruit 800 adults, ages 55 to 90, to participate in the research – approximately 200 cognitively normal older individuals to be followed for 3 years, 400 people with aMCI to be followed for 3 years, and 200 people with early AD to be followed for 2 years. For up-to-date information see *www.adni-info.org*.''

2.1.2. Study Sample. We considered 343 subjects with mild cognitive impairment (MCI) enrolled in the Alzheimer's Disease Neuroimaging Initiative (ADNI-1). These MCI patients were then followed over 48 months, with 150 participants progressing to AD (Table 1). MCI converters did not differ from MCI noncoverters in gender, handedness, marital status, retirement percentage, and age (p-values>0.05), but as expected, differed from them in APOE4 status as well as baseline cognition (p-value<0.05) (Table 1). Mean follow up time was 75 days longer in con-

verters (p=0.06). From them, we extracted high dimensional MR imaging and whole genome data, as well as routine neurocognitive and clinical data at baseline.

2.2 *MRI and Hippocampus Image Preprocessing*

2.2.1 MRI Image

These scans on 343 subjects were performed on a 1.5 T MRI scanners by using a sagittal MPRAGE sequence with the following parameters: repetition time (TR) = 2400 ms, inversion time (TI) = 1000 ms, flip angle = , and field of view (FOV) = 24 cm with a 256 256170 acquisition matrix in the x-, y-, and z-dimensions, which yields a voxel size of 1.251.261.2 .

We processed the MRI data by using standard steps including anterior commissure and posterior commissure correction, skull-stripping, cerebellum removing, intensity inhomogeneity correction, segmentation, and registration [40]. After segmentation, we segmented the brain data into four different tissues: grey matter (GM), white matter (WM), and cerebrospinal fluid (CSF). Moreover, we automatically labeled 93 ROIs on the Jacob atlas [21], and transferred the labels following the deformable registration of subject images [25]. In addition, we chose 23 ROIs, which may significantly influence MCI progression from the existing literature. [10][22][23] The 23 ROIs were bilateral entorhinal cortices, bilateral hippocampal formation, bilateral amygdala, bilateral caudate nuclei, bilateral putamen, bilateral posterior limb of internal capsule including cerebral peduncle, bilateral nucleus accumbens, bilateral lateral ventricles, bilateral thalamus, bilateral fornix, bilateral cingulate and the corpus callosum.

2.2.2 Hippocampus Image Preprocessing

We adopted a surface fluid registration based hippocampal subregional analysis package, [24] which uses isothermal coordinates and fluid registration to generate one-to-one hippocampal sur-

face registration for following surface statistics computation. This software package has been adopted by various studies [25-30].

Given the 3D MRI scans, hippocampal substructures were segmented with FIRST [31] and hippocampal surfaces were automatically reconstructed with the marching cube method [32]. We applied an automatic algorithm, topology optimization, to introduce two cuts on a hippocampal surface to convert it into a genus zero surface with two open boundaries. The locations of the two cuts were at the front and back of the hippocampal surface, representing its anterior junction with the amygdala, and its posterior limit as it turns into the white matter of the fornix. Then holomorphic 1-form basis functions were computed [33]. These induced conformal grids the hippocampal surfaces which were consistent across subjects. With this conformal grid, we computed the conformal representation of the surface [24], i.e., the conformal factor and mean curvature, which represent the intrinsic and extrinsic features of the surface, respectively. The "feature image" of a surface was computed by combining the conformal factor and mean curvature and linearly scaling the dynamic range into [0, 255]. Next, we registered the feature image of each surface in the dataset to a common template with an inverse consistent fluid registration algorithm. [26] With conformal parameterization, we essentially converted a 3D surface registration problem into a 2D image registration problem. The flow induced in the parameter domain establishes high-order correspondences between 3D surfaces. Finally, various surface statistics were computed on the registered surface, such as multivariate tensor-based morphometry (mTBM) statistics, [33] which retain the full tensor information of the deformation Jacobian matrix, together with the radial distance, [34] which retains information on the deformation along the surface normal direction.

2.3 The SNP data

The subjects' genotype variables were acquired based on the Human 610-Quad Bead- Chip (Illumina, Inc., San Diego, CA) in the ADNI database, which resulted in 620,901 SNPs. To reduce the population stratification effect, we used 749 Caucasians from all 818 subjects with complete imaging measurements at baseline. Quality control procedures included (i) call rate check per subject and per SNP marker, (ii) gender check, (iii) sibling pair identification, (iv) the Hardy-Weinberg equilibrium test, (v) marker removal by the minor allele frequency, and (vi) population stratification. The second line preprocessing steps include removal of SNPs with (a) more than 5% missing values, (b) minor allele frequency smaller than 5% , and (c) Hardy-Weinberg equilibrium p-value < 1e−6. Remaining missing genotype variables were imputed as the modal value. Seven hundred forty seven subjects and 504,095 SNPs remained.

We included information from all the 22 chromosomes. Since each chromosome contains a number of SNPs, we used principal component analysis for each chromosome and picked the first 2 principal components for each chromosome. We then used the PLINK package (https://pngu.mgh.harvard.edu/~purcell/plink/data.shtml#plink) to perform quality control for the genomic data. The principal component analysis for each chromosome was conducted using ``svd'' function in R software.

2.4 Statistical Approach

A popular model used in literature is the Cox proportional hazards model (Cox, 1972), which accounts for other covariates that are associated with the timing of the events. Covariates of interest include demographic information (8 covariates), the APOE4 genotype (3 covariates), the ADAS-Cog score (1 covariate), the hippocampus surface data (7 covariates for each curve, total 14 covariates), the ROI volume data (23 covariates), the chromosomewise information (2 covari-

ates for each chromosome, total 44 covariates) and the significant SNPs information (5 covariates). We used the R function "coxph" to implement the fitting of the Cox proportional hazards model. We fitted a Cox regression model with demographic, clinical and cognitive (ADAS-Cog score) predictors as well as APOE, referred to as the Clinical-Cognitive model (Model 1) from here on, and obtained its estimation and testing results. This model did not include any other imaging and genetic data. We fitted a second Cox regression model with demographic, imaging and chromosome-wise predictors, but without the ADAS-Cog score and significant SNPs information, referred to as the Imaging-Genetics model (Model 2) from here on, and obtained its estimation and testing results.

As a comparison, we also used the results obtained from Genome-wide Association Analysis (GWAS) to incorporate the genetic information. Specifically, we selected the top 101 significant SNPs by using a kernel machine method, [36] and then calculated their top 5 PCs and used them as predictors (significant SNP information). We fitted a third Cox regression model with demographic, imaging and significant SNP information, but without the ADAS-Cog score and chromosome-wise information, and then obtained parameter estimation and testing results. We referred this model to as the Traditional Imaging-Genetics Model (Model 3) from now on.

When we fitted Cox regression models, we treated the left and right hippocampus surface data as functional predictors. For each subject, the radial distance was obtained from baseline hippocampal surfaces data, which yields two 15000 dimensional vectors denoting data from left hippocampus and right hippocampus, respectively. We applied functional principal component analysis (FPCA) [38][39]. We selected 7 functional principal component (FPC) scores for each

functional predictor, which explain approximately 70% of the variance. For implementation of FPCA, we use the "svd" function in R software.

We used FPCA to extract the first seven FPCs of each of the left and right hippocampus surface data and the first two FPCs of the SNP data along each chromosome, then used theses as basis functions to represent the regression coefficient functions associated with the hippocampus surface and SNP on all chromosomes in the Cox regression. As an illustration, we plotted the first seven FPCs for both left and right hippocampi in Figure 1.

Since we do not have the validation data set, we investigated the predictive performance of the candidate models using the receiving operating characteristic (ROC) curve. In particular, we calculated the area under the curve (AUC), which is often used to measure the prediction of survival models. In particular, we first randomly picked 200 subjects for the training data and fit all the candidate models. After that, we used the remaining 143 individuals for the testing and calculated the AUC.[35] The method can be implemented by using the R function "AUC.cd". We repeated the above steps for 100 times, i.e. randomly separated the data for 100 times and obtained 100 AUCs. The mean and standard deviations can be obtained using these 100 AUCs.

3. Results

We compared the predictive value of standard of care (clinical demographic variables, APOE4, the ADAS-Cog score, Model 1) versus imaging-genetic markers (MRI volumes and surface data plus GWAS SNP and demographics, Model 2). We have obtained the first five principal components of the 101 top SNPs obtained from GWAS and add it into our Model 2 (call it

Model 3). We have compared our Model 2 versus Model 3 as well.

Receiver operating characteristic (ROC) analysis revealed that Model 1 (combining just routine clinical demographics and cognitive data with a single genotype ApoE4) had a low predictive value at 48 months (AUC 0.75) (Figure 2, Supplemental Table 1, Supplemental Figure 3). In this model, ApoE4 and ADAS-Cog were the significant predictors. In contrast, Model 2 (combining full genetic SNP and high dimension imaging data with demographics but without any cognitive data) had a much higher predictive value (AUC 0.95) (Figure 2, Supplemental Table 2, Supplemental Figure 3). SNPS on chromosome 2, 10, 11, 15, 17 and 18 (Supplemental Figure 2), ApoE4 status, surface morphology data of both hippocampi (especially anterior regions, Figure 1, Supplemental Figure 1) and volumes of hippocampus, amygdala and thalamus contributed significantly. The 100-fold cross validation using a test and training data set revealed AUC of 0.95 (+/-0.014) for the imaging-genetic model and 0.75 (+/-0.024) for the clinical-cognitive model. For the Traditional Imaging-Genetics model, we can only obtain a predictive value (AUC 0.90) (Figure 2, Supplemental Table 3, Supplemental Figure 3), which indicates the advantages of using the chromosome-wise information instead of the traditional significant SNPs information. The reason may be due to the pitfalls of prediction using significant SNPs.[37] Meanwhile, we have found that combining all variables (cognitive data plus imaging-genetic data) showed high predictive accuracy (AUC 0.96) but was not different from the value provided by imaging-genetics data alone. Besides, combining the significant SNPs information with all the predictors in our Imaging Genetics Model achieves slightly higher predictive accuracy (AUC 0.97), but was not different from the value provided by Imaging-Genetic Model alone.

From the estimation results of our imaging-genetics model, we have found that divorced individuals, the older people, individuals with 2nd allele of APOE4 genotype 3 may have smaller hazard function. The individuals with larger ROI volumes in hippocampal left, amygdala right

and thalamus left may have smaller hazard function, while the individuals with larger ROI volumes in hippocampal right, amygdala left, posterior limb of internal capsule and thalamus right may have larger hazard function.

4. Discussion

These findings are the first demonstration, to our knowledge, of the value of combined whole brain MR and whole genome SNP data in the 48-month prognosis of subjects at risk for AD. Our finding support prior MRI studies of volumetric hippocampal changes in prodromal AD [8][18] and extend them by finding that the possible prognostic value of combining information from high dimensional imaging and genetics may be superior to that provided by routine clinical-cognitive testing data.

Our findings also confirm the association between APOE4 status and AD, and identify additional new markers on chromosomes 2, 10, 11, 15, 17 and 18 as having significant effects on conversion. A variety of genes have been identified in prior GWAS studies as potential risk factors for AD such as clusterin (chromosome 8), complement receptor 1 (chromosome 1), phosphatidylinositol binding clathrin assembly protein (chromosome 11), sortilin-related receptor (chromosome 11), triggering receptor expressed on myeloid cells 2 (chromosome 6) and cluster of differentiation 33 (chromosome 19) as well as TOMM40 (chromosome 19).[19] Our study did not examine any of these newer gene markers specifically but provides support to the notion that there is additional genetic heritability in late-onset AD beyond that accounted for by APOE.

There are some strengths and limitations to our analyses. ADNI is a national biomarker study that utilized rigorous standardized data collection procedures, and well established criteria to select MCI subjects. Rather than using the individual data on all SNPs, we used the more conservative statistical method of doing principal component analysis for each chromosome and

picking the first 2 principal components for each chromosome. Our findings survived internal cross validation but need replication in an independent community based sample. We did not include measures of pathology (e.g. beta-amyloid) in our models since CSF and amyloid-PET were available only in a small subset of individuals in ADNI-1. However, a study of ADNI-2 subjects has shown a robust correlation between the APOE e4 ε4 allele and cortical amyloid burden [20], suggesting that APOE e4 may have served as a surrogate for cortical amyloid plaque load in our analysis. It is important to confirm the above findings obtained from ADNI-1 in other independent data sets [37].

Prior investigations of prediction of MCI-AD to AD have utilized feature selection to assess the most important biomarkers of prediction of conversion. Here, we have demonstrated the utility of Cox hazard models as a valuable method for identifying the "optimal combination" of early markers of conversion to AD in patients with MCI. If replicated in independent cohorts, such combinatorial markers of early AD could be useful for selecting at risk individuals for prevention trials and for discovering novel targets for discovering disease modifying therapies.

CONFLICT OF INTEREST

The authors declare no conflict of interest.

ACKNOWLEDGEMENTS

This work was supported in part by NlH grants RR025747-01, P01CA142538-01, MH086633, and AG033387 to Dr. Zhu. The content is solely the responsibility of the authors and does not necessarily represent the official views of the NIH. Data used in preparation of this article were obtained from the Alzheimer's Disease Neuroimaging Initiative (ADNI) database (adni.loni.usc.edu). As such, the investigators within the ADNI contributed to the design and implementation of ADNI and/or provided data but did not participate in analysis or writing of this report. A complete listing of ADNI investigators can be found at: http://adni.loni.usc.edu/wpcontent/uploads/how_to_apply/ADNI_Acknowledgement_List.pdf Data collection and sharing for this project was funded by the Alzheimer's Disease Neuroimaging Initiative (ADNI) (National Institutes of Health Grant U01 AG024904) and DOD ADNI (Department of Defense award number W81XWH-12-2-0012). ADNI is funded by the National Institute on Aging, the National Institute of Biomedical Imaging and Bioengineering, and through generous contributions from the following: Alzheimer's Association; Alzheimer's Drug Discovery Foundation; BioClinica, Inc.; Biogen Idec Inc.; Bristol-Myers Squibb Company; Eisai Inc.; Elan Pharmaceuticals, Inc.; Eli Lilly and Company; F. Hoffmann-La Roche Ltd and its affiliated company Genentech, Inc.; GE Healthcare; Innogenetics, N.V.; IXICO Ltd.; Janssen Alzheimer Immunotherapy Research & Development, LLC.; Johnson & Johnson Pharmaceutical Research & Development LLC.; Medpace, Inc.; Merck & Co., Inc.; Meso Scale Diagnostics, LLC.; NeuroRx Research; Novartis Pharmaceuticals Corporation; Pfizer Inc.; Piramal Imaging; Servier; Synarc Inc.; and Takeda Pharmaceutical Company. The Canadian Institutes of Health

Research is providing funds to support ADNI clinical sites in Canada. Private sector contributions are facilitated by the Foundation for the National Institutes of Health (www.fnih.org). The grantee organization is the Northern California Institute for Research and Education, and the study is coordinated by the Alzheimer's Disease Cooperative Study at the University of California, San Diego. ADNI data are disseminated by the Laboratory for Neuro Imaging at the University of Southern California.

PMD has received research grants and/or advisory fees from several government agencies, advocacy groups and pharmaceutical/imaging companies. PMD received a grant from ADNI to support data collection for this study and he owns stock in Sonexa, Maxwell, Adverse Events and Clarimedix, whose products are not discussed here.

REFERENCES

[1]. Michael W. Weiner, Dallas P. Veitcha, Paul S. Aisen, Laurel A. Beckett, Nigel J. Cairnsh, Robert C. Green, Danielle Harvey, Clifford R. Jack, William Jagust, Enchi Liu, John C. Morris, Ronald C. Petersen, Andrew J. Saykino, Mark E. Schmidt, Leslie Shaw, Judith A. Siuciak, Holly Soares, Arthur W. Toga, & John Q. Trojanowski; Alzheimer's Disease Neuroimaging Initiative. (2012). The Alzheimer's Disease Neuroimaging Initiative: A review of papers published since its inception. *Alzheimers Dement.*8, S1-S68.

[2]. Doraiswamy, P.M., Sperling, R.A., Johnson, K, Reiman, E.M., Wong ,T.Z., Sabbagh, M.N., Sadowsky, C.H., Fleisher, A.S., Carpenter, A, Joshi, A.D., Lu, M, Grundman, M, Mintun, M.A., Skovronsky, D.M., & Pontecorvo, M.J.; AV45-A11 Study Group. (2014) Florbetapir F 18 amyloid PET and 36-month cognitive decline:a prospective multicenter study. *Mol Psychiatry*, In Press.

[3]. Atluri G, Padmanabhan K, Fang G, Steinbach M, Petrella JR, Lim K, Macdonald A 3rd, Samatova NF, Doraiswamy PM, Kumar V. (2013) Complex biomarker discovery in neuroimaging data: Finding a needle in a haystack. *Neuroimage Clin.* 3:123-131.

[4]. Costafreda, S.G., Dinov, I.D., Tu, Z., Shi, Y., Liu, C.Y., Kloszewska, I., Mecocci, P., Soininen, H., Tsolaki, M., Vellas, B., Wahlund, L.O., Spenger, C., Toga, A.W., Lovestone, S., & Simmons, A. (2011) Automated hippocampal shape analysis predicts the onset of dementia in mild cognitive impairment. *Neuroimage.* **56**, 212-9.

[5]. Cui, Y., Liu, B., Luo, S., Zhen, X., Fan, M., Liu, T., Zhu, W., Park. M., Jiang, T., & Jin, S.E. (2011) Identification of conversion from Mild Cognitive Impairment to Alzheimer's disease using multivariate predictors. *PLoS One* **6**, e21896.

[6]. Cuingnet, R., Gerardin, E., Tessieras, J., Auzias, G., Lehericy, S., Habert, M.O., Chupin, M., Benali, H., & Colliot, O. Automatic classification of patients with Alzheimer's disease from structural MRI: a comparison of ten methods using the ADNI database. (2011) *Neuroimage* **56**, 766-81.

[7]. Davatzikos, C., Bhatt, P., Shaw, L.M., Batmanghelich, K.N., & Trojanowski, J.Q. Prediction of MCI to AD conversion, via MRI, CSF biomarkers, and pattern classification. (2011) *Neurobiol Aging* **32**, 2322.e19-2322.e27.

[8]. Dickerson, B.C. & Wolk., D. A., Alzheimer's Disease Neuroimaging Initiative. Biomarker-based prediction of progression in MCI: comparison of AD signature and hippocampal volume with spinal fluid amyloid-β and tau. (2013) *Front Aging Neurosci.* **5,** 1-9.

[9]. Eckerström C, Olsson E, Bjerke M, Malmgren H, Edman A, Wallin A, & Nordlund A. A combination of neuropsychological, neuroimaging, and cerebrospinal fluid markers predicts conversion from mild cognitive impairment to dementia. (2013) *J Alzheimers Dis.* **36**, 421-31.

[10]. Jack, C. R. Jr., Petersen, R. C., Xu, Y. C., et al Prediction of AD with MRI-based hippocampal volume in mild cognitive impairment. (1999) *Neurology **52,*** 1397-1403.

[11]. Qiu A., Fennema-Notestine, C., Dale, A.M., & Miller, M.I. (2009) Regional shape abnormalities in mild cognitive impairment and Alzheimer's disease. *Neuroimage* **45**,656-661.

[12]. Querbes, O., Aubry, F., Pariente, J., Lotterie, J.A., Demonet, J.F., Duret, V., Puel, M., Berry, I., Fort, J.C. & Celsis, P. (2009) Early diagnosis of Alzheimer's disease using cortical thickness: Impact of cognitive reserve. *Brain* **132.**

[13]. Shaffer, J.L., Petrella, J.R., Sheldon, F.C., Choudhury, K.R., Calhoun, VD, Coleman, RE, & Doraiswamy, P.M.; Alzheimer's Disease Neuroimaging Initiative. (2013) Predicting cognitive decline in subjects at risk for Alzheimer disease by using combined cerebrospinal fluid, MR imaging, and PET biomarkers. *Radiology* **266(2)**, 583-91.

[14]. Toledo JB, Weiner MW, Wolk DA, Da X, Chen K, Arnold SE, Jagust W, Jack C, Reiman EM, Davatzikos C, Shaw LM, Trojanowski JQ; Alzheimer's Disease Neuroimaging Initiative. (2014) Neuronal injury biomarkers and prognosis in ADNI subjects with normal cognition. *Acta Neuropathol Commun.* 2(1):26.

[15]. Young, J., Modat, M., Cardoso, M.J., Mendelson, A., Cash, D., & Ourselin, S. (2013) Accurate multimodal probabilistic prediction of conversion to Alzheimer's disease in patients with mild cognitive impairment. *Neuroimage Clin.* **2**,735-45

[16]. Zhang, D. & Shen, D. Predicting future clinical changes of MCI patients using longitudinal and multimodal biomarkers. (2012) *PLoS One* **7**(3).

[17]. Hohman TJ, Koran ME, Thornton-Wells TA; Alzheimer's Disease Neuroimaging Initiative. (2014)Genetic modification of the relationship between phosphorylated tau and neurodegeneration. *Alzheimers Dement.* pii: S1552-5260(14)00013-2.

[18]. Li, H, Liu, Y, Gong, P, Zhang, C, & Ye, J; Alzheimers Disease Neuroimaging Initiative. Hierarchical interactions model for predicting Mild Cognitive Impairment (MCI) to Alzheimer's Disease (AD) conversion. (2014) *PLoS One* **9(1)**:e82450.

[19]. Bagyinszky E, Youn YC, An SS, Kim S. (2014) The genetics of Alzheimer's disease. *Clin Interv Aging* 9:535-51.

[20]. Murphy KR, Landau SM, Choudhury KR, Hostage CA, Shpanskaya KS, Sair HI, Petrella JR, Wong TZ, Doraiswamy PM; Alzheimer's Disease Neuroimaging Initiative. (2013) Mapping the effects of ApoE4, age and cognitive status on 18F-florbetapir PET measured regional cortical patterns of beta-amyloid density and growth. *Neuroimage* 78:474-80.

[21]. Bryant, C., Giovanello, K. S., Ibrahim, J. G., Chang, J., Shen, D., Peterson, B. S., ... & Alzheimer's Disease Neuroimaging Initiative. (2013). Mapping the Genetic Variation of Regional Brain Volumes as Explained by All Common SNPs from the ADNI Study. *PloS one*, *8*(8), e71723.

[22]. Fennema‐Notestine, C., Hagler, D. J., McEvoy, L. K., Fleisher, A. S., Wu, E. H., Karow, D. S., & Dale, A. M. (2009). Structural MRI biomarkers for preclinical and mild Alzheimer's disease. *Human brain mapping*, *30*(10), 3238-3253.

[23]. Ryan, N. S., Keihaninejad, S., Shakespeare, T. J., Lehmann, M., Crutch, S. J., Malone, I. B., ... & Fox, N. C. (2013). Magnetic resonance imaging evidence for presymptomatic change in thalamus and caudate in familial Alzheimer's disease. *Brain*, *136*(5), 1399-1414.

[24]. Shi,J.,Wang,Y.,Ceschin,R.,An,X.,Lao,Y.,Vanderbilt,D.,Nelson,M.D., Thompson, P. M.,

Panigrahy, A. and Lepor e, N. (2013b). A multivariate surface- based analysis of the putamen in premature newborns: Regional differences within the ventral striatum. PloS One 8 e66736.

[25]. Wang, Y., Song, Y., Rajagopalan, P., An, T., Liu, K., Chou, Y.-Y., Gutman, B., Toga, A. W. and Thompson, P. M. (2011). Surface-based TBM boosts power to detect disease effects on the brain: an N= 804 ADNI study. Neuroimage 56 1993–2010.

[26]. Shi, J., Thompson, P. M., Gutman, B. and Wang, Y. (2013a). Surface fluid registration of conformal representation: Application to detect disease burden and genetic influence on hippocampus. NeuroImage 78 111–134.

[27]. Shi, J., Lepor, N., Gutman, B. A., Thompson, P. M., Baxter, L. C., Caselli, R. L., Wang, Y. and for the Alzheimer's Disease Neuroimaging Ini- tiative (2014). Genetic influence of apolipoprotein E4 genotype on hippocampal morphometry: An N = 725 surface-based Alzheimer's disease neuroimaging initiative study. Human Brain Mapping.

[28]. Monje, M., Thomason, M. E., Rigolo, L., Wang, Y., Waber, D. P., Sal- lan, S. E. and Golby, A. J. (2013). Functional and structural differences in the hippocampus associated with memory deficits in adult survivors of acute lymphoblastic leukemia. Pediatric Blood & Cancer 60 293–300.

[29]. Colom, R., Stein, J. L., Rajagopalan, P., Mart ınez, K., Hermel, D., Wang, Y., A lvarez-Linera, J., Burgaleta, M., Quiroga, M., Shih, P. C. and Thompson, P. M. (2013). Hippocampal structure and human cognition: Key role of spatial processing and evidence supporting the efficiency hypothesis in females. Intelligence 41 129–140.

[30]. Luders, E., Thompson, P. M., Kurth, F., Hong, J. Y., Phillips, O. R., Wang, Y., Gutman, B. A., Chou, Y. Y., Narr, K. L. and Toga, A. W. (2013). Global and regional alterations of hippocampal anatomy in long-term meditation practitioners. Human Brain Mapping 34 3369–3375.

[31]. Patenaude, B., Smith, S. M., Kennedy, D. N. and Jenkinson, M. (2011). A Bayesian model of shape and appearance for subcortical brain segmentation. Neu- roimage 56 907–922.

[32]. Lorensen, W. E. and Cline, H. E. (1987). Marching cubes: A high resolution 3D surface construction algorithm. In ACM Siggraph Computer Graphics 21 163–169. ACM.

[33]. Wang, Y., Zhang, J., Gutman, B., Chan, T. F., Becker, J. T., Aizen- stein, H. J., Lopez, O. L., Tamburo, R. J., Toga, A. W. and Thompson, P. M. (2010). Multivariate tensor-based morphometry on surfaces: application to mapping ventricular abnormalities in HIV/AIDS. NeuroImage 49 2141–2157.

[34]. Pizer, S. M., Fritsch, D. S., Yushkevich, P. A., Johnson, V. E. and Chaney, E. L. (1999). Segmentation, registration, and measurement of shape variation via image object shape. IEEE Transactions on Medical Imaging 18 851–865

[35]. Champless, L.E. and Diao, G. (2006). Estimation of time-dependent area under the curve for long-term risk prediction. Statistics in Medicine 25 3474-3486

[36]. Liu, X., Cai T., Wu, MC., Zhou, Q., Liu, G., Christiani, DC., and Lin, X. (2011). Kernel machine SNP-set analysis for censored survival outcomes in genome-wide association studies. Genetic Epidemiology, 35 620-31.

[37]. Wray, NR., Yang, J., Hayes, BJ., Price, AL., Goddard, ME. and Visscher, PM. (2013) Pitfalls of predicting complex traits from SNPs. Nature Reviews Genetics 14(7) 507-15

[38]. Rice, J.A. and Silverman, B.W. (1991). Estimating the mean and covariance structure nonparametrically when the data are curves. Journal of the Royal Statistical Society: Series B (Statistical Methodology) 53 233-243.

[39]. Ramsay, J.O. and Silverman, B.W. (2005). Functional Data Analysis. 2nd ed. Springer Series in Statistics, Springer, New York.

[40]. Shen, D.G., Davatzikos, C.: Measuring temporal morphological changes robustly in brain mr images via 4-dimensional template warping. NeuroImage 21, 1508–1517 (2004).

FIGURE LEGENDS

Figure 1. Figure presents the estimated coefficient functions associated with the hippocampus surface data. Panel (a)-(g) are the estimates of the first seven FPCs corresponding to the sorted seven eigenvalues, in which panel (a) corresponds the largest eigenvalue, and Panel (h) is the color bar with 11 lines representing 11 equally spaced points between [-0.0462, 0.0421].

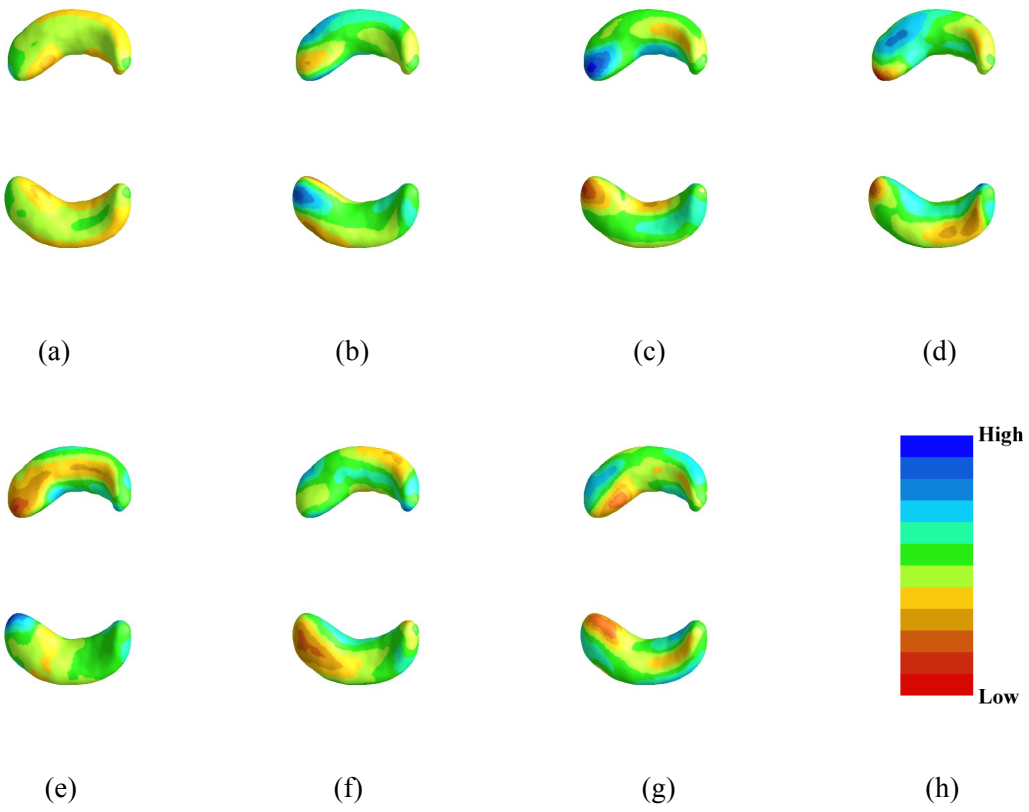

Figure 1. Figure presents the estimated coefficient functions associated with the hippocampus surface data. Panel (a)-(g) are the estimates of the first seven FPCs corresponding to the sorted seven eigenvalues, in which panel (a) corresponds the largest eigenvalue, and Panel (h) is the color bar with 11 *lines representing 11 equally spaced points between [-0.0462, 0.0421].*

Figure 2. The ROC curves comparison for the imaging plus genetics model versus the cognitive model plotted using one pair of training and testing data set. The blue solid line denotes the ROC curve for the image-genetics model and the red dash line denotes the ROC curve for clinical-cognitive model.

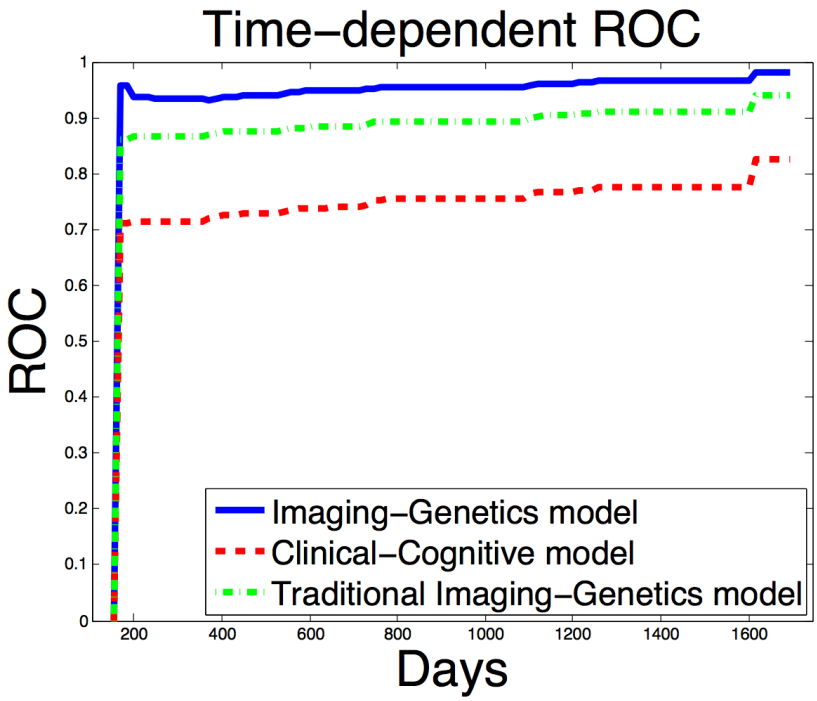

Figure2: The ROC curves comparison for the imaging plus genetics model versus the cognitive model plotted using one pair of training and testing data set. The blue solid line denotes the ROC curve for the imaging-genetics model, the red dash line denotes the ROC curve for clinical-cognitive model and the green dash dot line denotes the ROC curve for the traditional imaging-genetics model.

Table 1: Study sample –Comparison of Converters and Nonconverters

	MCI converters	MCI noncon-verters	Test statistics
Sample Size	150	193	
Mean Age (in years)	74.7 (7.0)	75.1 (7.5)	T test: Pvalue=0.69
Gender (Male percentage)	60.0%	66.8%	Chi-square test: Pvalue=0.23
Handedness (Right hand percentage)	92.0%	90.7%	Chi-square test: Pvalue=0.81
Marital Status (Widowed percentage)	10.7%	11.9%	Chi-square test: Pvalue=0.95
Marital Status (Divorced percentage)	4.7%	6.2%	
Marital Status (Never Married per-centage)	1.3%	1.0%	
Mean Education Length (in years)	15.6 (2.9)	15.8 (3.0)	T test: Pvalue=0.52
Retirement percentage	80.0%	79.3%	Chi-square test: Pvalue=0.98
APOE 4 carriers (%) : APOE4 first allele (genotype 3 percentage)	78.7%	81.4%	Chi-square test: Pvalue=0.02
APOE4 first allele (genotype 4 per-centage)	17.3%	9.3%	

APOE4 second allele (genotype 4 percentage)	30.0%	56.0%	Chi-square test: Pvalue<0.0001
Mean ADAS-Cog 11 Score	13.2 (4.0)	10.2 (4.3)	T test: Pvalue<0.0001
Mean Duration of Follow up (in days)	1009.9	934.4	T test: Pvalue=0.06